Numerical study of the effect of heat transfer on solid phase formation during decompression of CO_2 in pipelines

Sergey Martynov, *Wentian* Zheng, and *Haroun* Mahgerefteh*

Department of Chemical Engineering, University College London, WC1E 7JE, London, UK

Abstract. CO_2 solid phase formation accompanying rapid decompression of high-pressure CO_2 pipelines may lead to blockage of the flow and safety valves, presenting significant hazard for safe operation of the high-pressure CO_2 storage and transportation facilities. In this study, a homogeneous equilibrium flow model, accounting for conjugate heat transfer between the flow and the pipe wall, is applied to study the CO_2 solid formation in a 50 mm internal diameter and 37 m long pipe for various initial thermodynamic states of CO_2 fluid and wide range of discharge orifice diameters. The results show that the rate of CO_2 solid formation in the pipe is limited by heat transfer at the pipe wall. The predicted amounts of solid CO_2 are discussed in the context of venting of CO_2 pipelines.

1 Introduction

Despite the fact that carbon dioxide (CO_2) at low concentrations is commonly considered as a safe substance, accidental failure of facilities transporting large quantities of CO_2 at high pressures for carbon capture and storage or utilization [1,2] may cause significant harm to personnel and local populations as a result of explosion overpressure and the asphyxiate nature of the CO_2 in the ensuing dispersion cloud [3,4].

Blockage of safety valves by solid CO_2 which may form as a result of near-isentropic decompression of high-pressure CO_2 to the level below 5.18 bar (triple point of CO_2) is considered as one of major causes of failure of CO_2 storage and transport facilities [5,6]. Also, accumulation of solid CO_2 in pipelines and vessels may increase the risk of blockage and overfilling of units at later stages of operation [7–11]. In particular, our recent studies showed that solid CO_2 may form during decompression of pipelines initially filled with CO_2 at 60-80 bar pressures [12,13]. Given that solid CO_2 accumulation in safety valves and vented sections of pipelines presents a risk for the system integrity, designing venting equipment and procedures that minimize the amounts of solid phase formed becomes critically important. This requires development and application of mathematical models of pipeline decompression accounting for multiphase nature of the decompression flow and thermodynamic properties of CO_2 fluid in various states, including the triple point.

Recent studies showed that Homogeneous Equilibrium Mixture (HEM) model predicts well the pressure and temperature measured in the pipeline Full Bore Rupture test [13] and amounts of solid CO_2 formed in the pipeline in the orifice discharge tests [12]. Using this model it was demonstrated that duration of the pipeline decompression to the triple point where CO_2 solids can form in the pipe, scales with the pipeline length [14], while the amount of solid CO_2 formed depends on the history of decompression flow [12]. The latter depends on a number of factors, including the initial thermodynamic state of the fluid, the discharge hole diameter, and the rate of heat transfer at the pipe wall. Despite the fact that understanding the above effects is crucial for preventing/minimizing the CO_2 solids formation in process equipment, they have not been systematically studied. The present study is focused on the application of the HEM flow model to quantify the amount of CO_2 solid phase that may form under various scenarios of pipeline decompression..

* Corresponding author: h.mahgerefteh@ucl.ac.uk

2 Theory

In the present study, in order to predict the history of decompression of a CO_2 pipeline (Figure 1) accounting for spatial variations in the flow along the pipe, a set of quasi-one-dimensional HEM-based mass, momentum and energy conservation equations, is applied [15]:

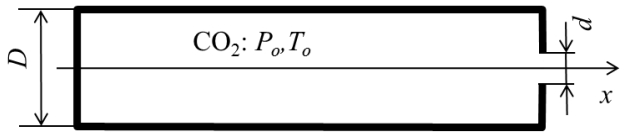

Fig. 1. Schematics of a pipeline filled with CO2 at pressure Po and temperature To prior to decompression through an orifice of diameter d.

$$\frac{\partial}{\partial t}\rho A+\frac{\partial}{\partial x}\rho uA=0 \quad (1)$$

$$\frac{\partial}{\partial t}\rho uA+\frac{\partial}{\partial x}(\rho u^2+p)A=p\frac{\partial A}{\partial x}-2f\rho u^2\frac{A}{D} \quad (2)$$

$$\frac{\partial}{\partial t}\left(u^2/2+e\right)\rho A+\frac{\partial}{\partial x}\left[\rho\left(u^2/2+e\right)+p\right]uA= =\left(-2f\rho u^3+4q\right)\frac{A}{D} \quad (3)$$

where p is the pressure, u is the velocity, D and $A=\pi D^2/4$ are respectively the pipe diameter and cross-sectional area of the flow; f is the Fanning friction factor, calculated using Chen's correlation [16], and q is the heat flux at the pipe wall.

In the above equations, the HEM density and specific internal energy are calculated knowing the fluid phase composition and properties of saturated vapor, liquid and solid phases as functions of pressure. The thermodynamic properties of CO_2 in liquid and vapor states are calculated using the GERG 2004 equation of state (EoS) [17], while properties of solid CO_2 are predicted using the extended Peng-Robinson EoS [18].

The heat flux, q, is defined by Newton's cooling law for single-phase and solid-vapor turbulent flows (with the Dittus-Boelter correlation [19] adopted to predict the heat transfer coefficient), and using Rohsenow's correlation for nucleate boiling [20] for vapor-liquid flows.

The set of equations (1) - (3) is closed by the boundary conditions specified at both ends of the pipeline (Figure 1), and using a lumped heat capacity model predicting evolution of the pipe wall temperature [14].

For the numerical solution of the governing equations of the model, Godunov's finite volume method combined with a fractional stepping time-integration scheme is applied [21].

At any time level, the total amount of CO_2 solid phase formed in the pipe is obtained by numerically integrating the resolved solid phase density profiles along the pipeline. The time integration procedure is terminated when the pressure at the discharge end of the pipe reaches 1 bar.

3 Results and discussion

This section is aimed at evaluation of the impact of key parameters of decompression process on the solid CO_2 formation in pipelines. For this purpose, the above described model is applied to predict the amount of solid CO_2 formed in a pipe for various initial states of CO_2 fluid and various discharge orifice diameters. For the sake of example, the study is performed for a medium-scale mild steel pipeline of 50 mm internal diameter, 5 mm wall thickness and 37 m length (http://www.co2quest.eu/).

3.1 The effect of initial conditions

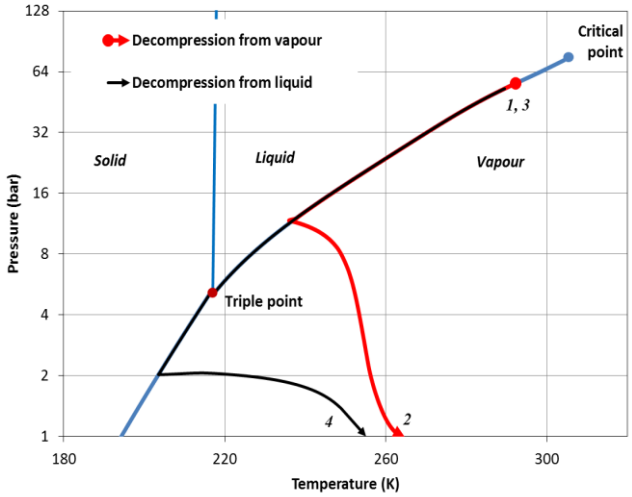

Fig. 2. Pressure-temperature phase diagrams of CO_2, showing the decompression trajectories predicted by the flow model for the fluid initially in the vapor state (trajectory *1-2*) and in the liquid state (trajectory 3-4).

In order to demonstrate the impact of initial conditions on the amount of solid CO_2 that could form in the pipe, the study was performed for two cases involving depressurization of the pipeline, initially at 54.4 bar pressure and 18 ^oC, via 6 mm orifice. In the first case the pipeline was initially filled with saturated liquid, while in the second case the pipe contained compressed saturated gas.

In Figure 2 evolution of the fluid pressure and temperature predicted by the model at location in the middle of the pipe, are plotted in the phase diagram of

CO_2. As can be seen in Figure 2, the liquid phase decompression path (trajectory *3-4*) crosses the triple point, and hence corresponds to a scenario where CO_2 solids can be expected to form in the pipe. At *ca.* 2 bar, the model predicts complete sublimation of the solid phase, and the trajectory deviates from the sublimation line into the vapor phase region. On the other hand, the decompression from the compressed gas state (trajectory *1-2*) follows the saturation line only till *ca.* 12 bar pressure, where the fluid turns to vapor, as can be explained by heating from the pipe wall. As such, the model indicates that decompression of a compressed CO_2 gas state doesn't lead to CO_2 solids forming in the pipe.

3.2 The effect of release orifice diameter

Figure 3 shows the effect of *d/D* ratio on the mass of solid CO_2 formed in the pipe upon its decompression to the triple point, obtained based on the HEM flow model predictions, in comparison with estimates using the thermodynamic method assuming isentropic decompression [12].

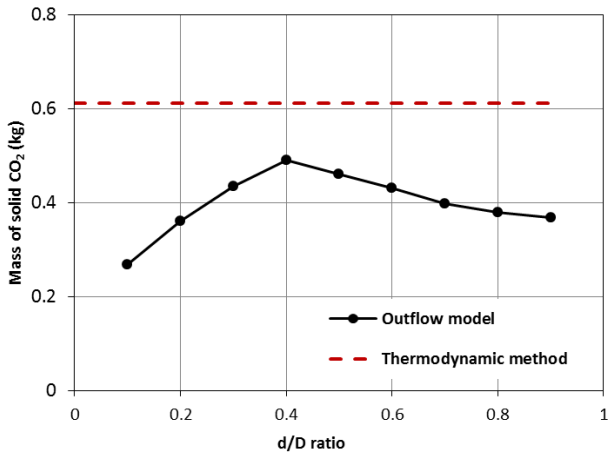

Fig. 3. The impact of the release orifice diameter on the amount of CO_2 solid phase formed in the pipeline, initially in liquid state at 18 ^{o} C and 54.4 bar.

As can be seen in Figure 3, predictions by the thermodynamic method are insensitive to the orifice diameter. Also, the thermodynamic method systematically (by *ca.* 15-50 %) overestimates the mass of solid phase in comparison with the predictions by the decompression flow model. This discrepancy can be directly attributed to non-isentropic nature of the fluid expansion process, involving conjugate heat transfer between the fluid and the pipe wall. Figure 3 also shows that the mass of solid CO_2 predicted by the outflow model scales nearly linearly with d/D in the range from 0.1 to 0.4. This indicates that using small ratios d/D can be more advantageous for use in design of decompression systems where the solid CO_2 pose hazard for the system operation and integrity.

4 Conclusions

The results obtained using the HEM pipeline outflow model showed that decompression of CO_2 from initial vapor state is characterized by significant heating of the flow by the pipe wall. This heating may result in complete evaporation of liquid phase before the fluid decompression to the triple point, leading to no CO_2 solids formed in the pipe. This contrasts to scenarios of decompression of pipes containing CO_2 in a form of compressed liquid, which evaporates only partially upon decompression to the triple point, potentially leading to large amount of solid CO_2 forming in the pipe, creating a hazard for the system operation and integrity.

The amounts of solid CO_2 calculated based on the simulations using the HEM flow model were compared with predictions using the thermodynamic model. While the latter gives conservative estimate of the amount of solid CO_2, the HEM decompression flow model resolves the effect of the orifice diameter and hence can become useful, *e.g.* for design of CO_2 venting systems.

Acknowledgments

The authors gratefully acknowledge the financial support provided by the European Union 7th Framework Program FP7-ENERGY-2012-1-2STAGE under grant agreement number 309102. The paper reflects only the authors' views and the European Union is not liable for any use that may be made of the information contained therein.

References

1 IPCC, *Carbon Dioxide Capture and Storage*, (Cambridge University Press, Cambridge, UK, 2005)

2 Styring P, Jansen D, de Coninck H, Reith H, Armstrong K, *Carbon Capture and Utilisation in the Green Economy* (The Centre for Low Carbon Futures and CO2 Chem Publishing, 2011)

3 Harper P, Wilday J, Bilio M, *Assessment of the Major Hazard Potential of Carbon Dioxide (CO_2)*, 2011.

4 M. van der Voort, A. van den Berg, D. Roekaerts, M., Xie, and P. de Bruijn, 2012, Shock Waves, **22**, pp. 129–140.

5 D. Huang, H. Quack, and G. Ding, 2007, Appl. Therm. Eng., **27**, pp. 1911–1922.

6 W. Clayton, and M. Griffin, 1994, Process Saf. Prog., **13**(4), pp. 202–209.

7 DNV, 2010, *Design and Operation of CO2*

Pipelines. Recommended Practice DNV-RP-J202.

8 Chart Inc., 2014, *CO_2 Storage Tank - Product Manual*, New Prague, MN 56071 USA.

9 M. Kim-E, 1981, "The Possible Consequences of Rapidly Depressurizing a Fluid," Massachusetts Institute of Technology.

10 Emerson Climate Technologies, 2015, *Commercial CO_2 Refrigeration Systems. Guide for Subcritical and Transcritical CO_2 Applications*.

11 D. Huang, G.. Ding, H. Quack, 2008, Front. Energy Power Eng. China, **2**(4), pp. 494–498.

12 S. Martynov, W. Zheng, H. Mahgerefteh, S.Brown, J. Hebrard, D. Jamois, C. Proust, 2018, Ind. Eng. Chem. Res., **57**, pp. 7054–7063.

13 W. Zheng, H.Mahgerefteh, S. Martynov, S. Brown, 2017, Ind. Eng. Chem. Res., **56**, pp. 10491–10499.

14 S. Martynov, S., Brown, H., Mahgerefteh, V., Sundara, S., Chen, Y., Zhang, 2014, Process Saf. Environ. Prot., **92**(1), pp. 36–46.

15 S. Brown, S. Martynov, H. Mahgerefeth, 2015, Comput. Fluids, **120**, pp. 46–56.

16 N. Chen, 1979, Ind. Eng. Chem. Fundam., **18**(3), pp. 296–297.

17 O. Kunz, W. Wagner, 2012, J. Chem. Eng. Data, **57**(11), pp. 3032–3091.

18 Martynov, S., Brown, S, Mahgerefteh, H., 2013, Greenh. Gases Sci. Technol., **3**(2), pp. 136–147.

19 F. Dittus, and L.Boelter, 1930, University of California Press, Berkeley, California, p. 443.

20 Incropera F, De Witt D, *Fundamentals of Heat and Mass Transfer* (John Wiley & Sons, New York, 1985)

21 LeVeque R. J, *Finite Volume Methods for Hyperbolic Problems*, Cambridge Univ. Press, 2002)